NiO: Correlated Band Structure of a Charge-Transfer Insulator

J. Kuneš,[1,2,*] V. I. Anisimov,[3] S. L. Skornyakov,[4] A. V. Lukoyanov,[4] and D. Vollhardt[1]

[1]*Theoretical Physics III, Center for Electronic Correlations and Magnetism, Institute of Physics, University of Augsburg, Augsburg 86135, Germany*

[2]*Institute of Physics, Academy of Sciences of the Czech Republic, Cukrovarnická 10, 162 53 Praha 6, Czech Republic*

[3]*Institute of Metal Physics, Russian Academy of Sciences-Ural Division, 620041 Yekaterinburg GSP-170, Russia*

[4]*Ural State Technical University-UPI, 620002 Yekaterinburg, Russia*

(Received 11 May 2007; published 9 October 2007)

The band structure of the prototypical charge-transfer insulator NiO is computed by using a combination of an *ab initio* band structure method and the dynamical mean-field theory with a quantum Monte-Carlo impurity solver. Employing a Hamiltonian which includes both Ni d and O p orbitals we find excellent agreement with the energy bands determined from angle-resolved photoemission spectroscopy. This brings an important progress in a long-standing problem of solid-state theory. Most notably we obtain the low-energy Zhang-Rice bands with strongly $\mathbf{k}$-dependent orbital character discussed previously in the context of low-energy model theories.

DOI: 10.1103/PhysRevLett.99.156404 PACS numbers: 71.27.+a, 71.10.−w, 79.60.−i

The quantitative explanation of the electronic structure of transition-metal oxides (TMOs) and other materials with correlated electrons has been a long-standing challenge in condensed matter physics. While the basic concept explaining why materials such as NiO are insulators was formulated by Mott a long time ago [1], the development of an appropriate, material-specific computational scheme proved to be a formidable task. The electronic structure of the late TMOs, including the cuprate superconductors, is not only affected by the electronic correlations, it is further complicated by the hybridization between the transition-metal d states and O p bands located between the lower and upper Hubbard bands formed by the transition-metal d orbitals. For such materials Zaanen, Sawatzky, and Allen [2] introduced the term ''charge-transfer insulator'', a prototypical example of which is NiO. In principle, the simple crystal structure of NiO allows for a straightforward comparison between theory and experiment. However, a theoretical description of the NiO band structure is made difficult by the competition between the local many-body effects, due to strong Coulomb interaction between Ni d electrons, and the band dispersion, due to the lattice periodicity, both observed with the angle-resolved photoemission spectroscopy (ARPES) [3,4].

In this Letter we use a combination of a conventional band structure approach, based on the local density approximation (LDA), and the dynamical mean-field theory (DMFT) [5] to investigate the band structure of NiO. No adjustable parameters enter. While the application of the LDA + DMFT [6] framework has proven successful for the early TMOs, the charge-transfer materials were routinely avoided due to the additional complexity arising from the presence of p bands. In the present work the O p orbitals and their hybridization with Ni d orbitals are explicitly included, thus allowing for a unified description of the full spectrum. Our results reveal a nontrivial effect of the p-d hybridization in strongly correlated systems studied so far only in terms of simple models [7–9].

The application of the standard band structure theory to NiO is marked by the failure of LDA to produce an insulating groundstate [10]. The antiferromagnetic (AFM) solution within LDA [11], despite rendering NiO an insulator, still underestimates the band gap severely, does not reproduce the experimental single-particle spectrum and also many ground state quantities are outside the usual LDA margin (e.g., too low magnetic moment). Theoretical approaches beyond LDA followed several different paths. The LDA + U [12] and *SIC*-LDA theories [13], although different in details and reasoning, enforce energy separation of the occupied and unoccupied Ni-d orbitals, which leads to the opening of a gap. This is sufficient to largely improve the ground state properties such as the local moment or the lattice constant [14]. However, the description of photoemission spectra is not satisfactory, in particular, the d spectral weight is located mostly in the high-energy satellite (Hubbard band), in striking contrast to a strong d contribution at the low excitation energy (top of the valence band) observed experimentally. This failure can be traced to the static character of the theories, which also restricts their success to the insulating stoichiometric NiO (in contrast to doped metallic) and the broken symmetry phase (AFM order). Some improvement in description of the photoemission spectra was achieved by including three-body corrections [15]. A different approach to the electron-electron correlations in NiO is provided by *GW* approximation [16,17]. While the dispersion of d bands at the top of the valence band and the band gap compare quite well to the experiment, Aryasetiawan and Gunnarsson [16] have shown and explained why the high-energy satellite, which contains almost 50% of the d spectral weight, is completely missing in the *GW* approach. The exact diagonalization study on NiO small

clusters of Fujimori *et al.* [8], which captures the distribution of the d spectral weight between the high- and low-energy structures, provides a strong evidence for the importance of full dynamical treatment of the local electron-electron correlations. This is achieved in the present work by employing the numerically exact QMC algorithm to the local problem of Ni site [18]. In the previous work [19] we have shown how the dynamical correlations enforce the spectral weight distribution between the high-energy satellite and the low-energy bands as well as a nontrivial behavior of doped NiO. Here we discuss the k-resolved single-particle spectra.

A systematic inclusion of local dynamical correlations into lattice models was made possible by the DMFT [5], which neglects the intersite correlations, an approximation expected to be quite accurate in three-dimensional systems. The connection of DMFT with band structure methods, usually referred to as the LDA + DMFT scheme [6], provides access to material-specific quantities. LDA + DMFT calculation starts with construction of an effective Hamiltonian from the converged LDA band structure using a projection onto Wannier orbitals. A subtle part of the procedure is subtracting the d-d interaction already present in the LDA calculation, so called double-counting correction, which is not uniquely defined. Choice of a particular double-counting scheme may influence the details, but not the overall spectral features discussed here (for details see Ref. [19]). Typically only the transition-metal d bands are included in the construction, which amounts to integrating out O p states [20] at the price of having more extended Wannier orbitals, a procedure only justified for the early TMOs with low-lying p bands. In the present study we project Wannier states out of a single energy window including both p and d bands, resulting in a more localized O p and Ni d Wannier orbitals with mutual hybridization.

The self-consistent solution of the LDA + DMFT problem follows the procedure of Ref. [19]; in particular, the calculations were performed in the paramagnetic state (PM) at the temperature $T = 1160$ K. While it may appear paradoxical, it is more demanding to theoretically describe the electronic structure of the PM state than of the symmetry broken AFM state. It is now generally excepted that the gap opening in NiO is due to electronic correlations and thus survives in the PM state, and antiferromagnetism is merely a parasitic effect on top of it, a conclusion which has a strong support in the ARPES data of Tjernberg *et al.* [21] measured across the Néel temperature $T_N = 525$ K showing that the NiO band structure is largely insensitive to the magnetic order. Rather high temperature of the present calculation was dictated by technical feasibility of the study (note that with the present QMC algorithm the CPU time scales as $\frac{1}{T^3}$). Given the energy scales and approximations involved, especially missing dipolar matrix elements for the photoelectron excitation, we do not find the high temperature to present an important limitation. The d-spectral functions were obtained by the maximum entropy method [22] applied separately for the e_g and t_{2g} symmetry. The local self-energy $\Sigma(\omega^+)$, which is formally an 8×8 matrix with the only nonzero elements on the diagonal of dd block, is obtained by solving the equation

$$G_{dd}(\omega^+) = \sum_{\mathbf{k}} [\omega^+ + \mu - h_{\mathbf{k}} - \Sigma(\omega^+)]^{-1}_{dd}, \qquad (1)$$

simultaneously for e_g and t_{2g} symmetry. Here the G_{dd} is the diagonal element of the Green function corresponding to either e_g or t_{2g} symmetry, $h_{\mathbf{k}}$ is the 8×8 Hamiltonian matrix on a mesh of $\mathbf{k}$-points and μ is the self-consistently determined chemical potential. The equation is solved approximately on the contour $\mathrm{Im}\omega^+ = 0.05$ eV subject to the constraints $\mathrm{Im}\Sigma(\omega^+) < 0$ and Kramers-Kronig relations, which are, however, satisfied automatically for good quality QMC data.

In Figs. 1 we compare the theoretical bands, represented by the $\mathbf{k}$-dependent spectral density $A(\mathbf{k}, \omega)$, along the Γ-X and Γ-K lines in the Brillouin zone with ARPES data of Refs. [3,4]. Both theory and experiment exhibit two relatively flat bands at -2 and -4 eV followed by several dispersive bands in the -4 to -8 eV range and a broad

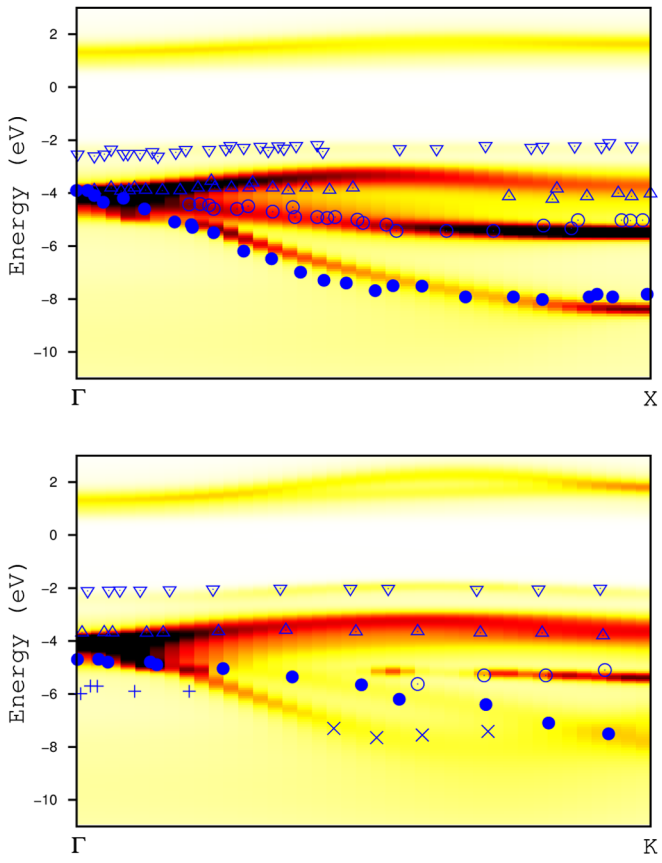

FIG. 1 (color online). The $\mathbf{k}$-resolved total spectral function $A(\mathbf{k}, \omega)$ along the Γ-X (upper panel) and Γ-K (lower panel) lines in the Brillouin zone depicted as a contour plot. The symbols represent the experimental bands of Shen *et al.* [4]. The theoretical gap edge was aligned with the experimental one.

incoherent peak around −10 eV. Overall we find an excellent agreement. The deviations around the Γ point in the lower panel of Fig. 1 are due to the inaccuracy in the location of the Γ point in off-normal-emission experiment [4]. The crosses near the Γ point mark a weak band which was interpreted as a consequence of AFM order [4] and is therefore not expected to be found in the paramagnetic phase investigated here. Additional weak structures in the uppermost valence band (not shown here) were identified in the spectra of Ref. [4]. To assess their importance the reader is kindly referred to the original experimental spectra. In Fig. 2 we show the orbital decomposition $A_{\nu\nu}(\mathbf{k}, \omega)$ of the spectral density visualized as a shape-preserving function $\frac{A_{\nu\nu}(\mathbf{k},\omega)}{C+A_{\nu\nu}(\mathbf{k},\omega)}$, in order to capture both sharp and broader features in a single plot.

We start the discussion of our results by considering the limit of vanishing p-d hybridization, in which case the entire d spectral weight is located in more or less featureless Hubbard bands located below the p-band manifold [19] and the holes in the uncorrelated p bands have infinite lifetimes. The p-d hybridization changes this picture qualitatively. In particular, two additional bands of mixed character appear at −2 and −4 eV of Fig. 1. These bands contain about half of the valence d-spectral weight as can

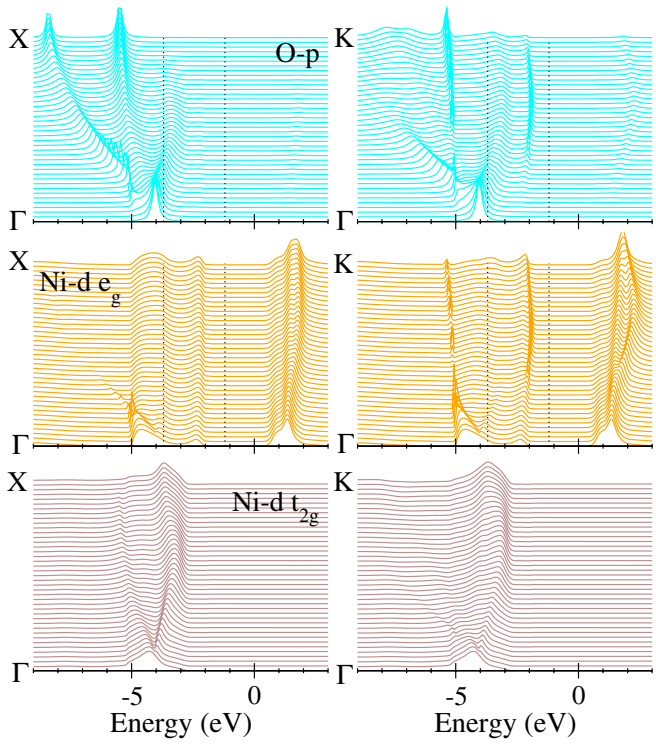

FIG. 2 (color online). The orbitally decomposed spectral function $A_{\nu\nu}(\mathbf{k}, \omega)$ along the Γ-X (left column) and Γ-K (right column) lines in the Brillouin zone plotted as $\frac{A_{\nu\nu}(\mathbf{k},\omega)}{C+A_{\nu\nu}(\mathbf{k},\omega)}$. The panels from top to bottom show the O-p, Ni-$d - e_g$, and Ni-$d - t_{2g}$ contributions. Here $C = 1.5$, 2 for the p and d projections, respectively. Detail of the uppermost valence band marked by the dotted lines is shown in Fig. 3.

be seen from the **k**-integrated spectrum of Ref. [19]. In addition, the lower Hubbard band is broadened due to the opening of the p-d decay channel for the d-holes introducing a pronounced asymmetry between the upper and lower Hubbard bands (see the middle panel of Fig. 2). (Compare to the symmetric upper and lower Hubbard bands of the e_g symmetry in Fig. 3 of Ref. [20], where p-d hybridization was not included.) Reciprocally, the p bands possess a finite **k**-dependent width due to the coupling to the correlated d bands. While full quantitative comparison to the ARPES data is not possible because of missing dipole matrix elements, the **k**-dependent broadening of the p bands (see the upper panel of Fig. 2) agrees well with the experimental observations [3,4]. In particular, we point out the broadening of the otherwise sharp p bands observed around the midpoint of the Γ-X line and a considerable smearing of the lowest two p bands near the K point (upper right panel of Fig. 2), which are hardly recognizable in the experimental spectra.

The low-energy bands of charge-transfer systems, especially in the case of high temperature cuprate superconductors, have been subject of numerous theoretical investigations. This was initiated by Zhang and Rice [7] who constructed an effective t-J Hamiltonian for holes doped to the copper-oxygen plane and who introduced the notion of a bound state between the p hole and d spin known as the Zhang-Rice singlet. Using a canonical transformation of the Hubbard model onto the spin-fermion model, Eroles *et al.* [23] found a strong **k**-dependence in the orbital composition of the Zhang-Rice band. Bała *et al.* [24,25] applied a generalized spin-fermion model to a 2D slab of NiO and obtained qualitative agreement with the corresponding part of the ARPES spectrum. They found very strong **k**-dependence of the spectral weight in the uppermost valence band. To a good approximation the latter corresponds to the p-spectral weight of the original multiband Hubbard model [23] and is thus directly comparable to the results of the present study. Like Bała *et al.*, we find a vanishing p-spectral weight in the uppermost valence band along the Γ-X ($\langle 11\rangle$ in Ref. [24]) line as well as a substantial p contribution in the Γ-K direction ($\langle 10\rangle$ in Ref. [24]) shown in Fig. 3. In addition, we find a rather **k**-independent d contribution to the uppermost valence band, which was suggested in Ref. [25] and which reflects the local character of the Zhang-Rice bound state, a doublet in the case of NiO. Unlike model theories, which are restricted to a special part of the Hilbert space, the LDA + DMFT scheme provides a unified picture of all energy scales and avoids any adjustable parameters. The good agreement with the experimental data and the low-energy model theory found in this work demonstrates the capability of DMFT to adequately describe charge-transfer systems and puts the earlier model results on a solid foundation.

In conclusion, by employing dynamical mean-field theory combined with LDA electronic structure calculation

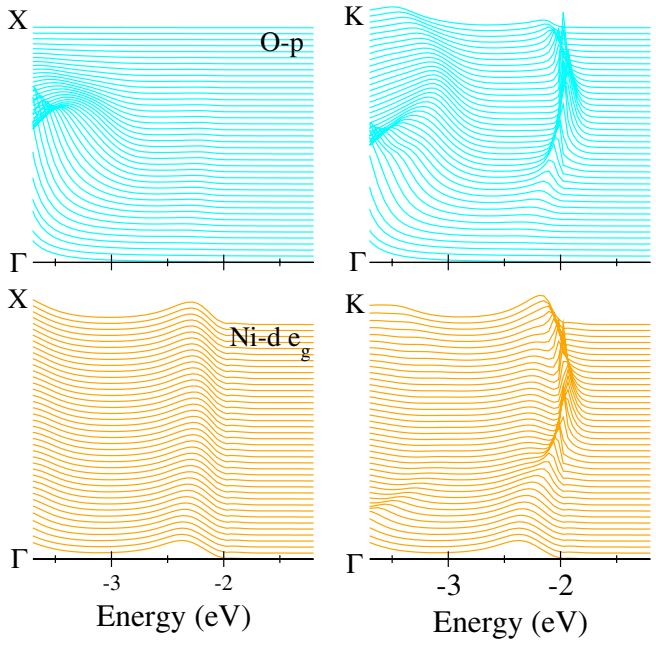

FIG. 3 (color online). Detail of the uppermost valence band along the Γ-K (right) and Γ-X (left) lines. The top panels show the O-p contribution $A_{pp}(\mathbf{k}, \omega)$, while Ni-$d$ contribution $A_{dd}(\mathbf{k}, \omega)$ $A_{dd}(\mathbf{k}, \omega)$ of the e_g symmetry is shown in the bottom panels.

we presented an important advance in a long-standing problem—the computation of the full valence band structure of a charge-transfer insulator. We obtained a very good agreement with the ARPES data of Shen *et al.* [3,4] without adjustable parameters. While a detailed comparison to ARPES data is still restricted by the lack of dipolar matrix elements in the theory, the key problem of the NiO spectrum, distribution of d-spectral weight between the high-energy satellite and the low-energy bands, was resolved. The uppermost valence band is found to have a strongly $\mathbf{k}$-dependent orbital composition, which follows the behavior expected of Zhang-Rice bands. Our results clearly demonstrate the capability of DMFT to treat, upon explicit inclusion of p-d hybridization, the late transition-metal oxides and charge-transfer systems in general.

J. K. gratefully acknowledges the Alexander von Humboldt Foundation for support. This work was supported by the SFB 484 of the Deutsche Forschungsgemeinschaft (J. K., D. V.), by the Russian Foundation for Basic Research under the Grants No. RFFI-06-02-81017, No. RFFI-07-02-00041 (V. I. A., S. L. S., and A. V. L.) and by the Dynasty Foundation (A. V. L.).

*jan.kunes@physik.uni-augsburg.de

[1] N. F. Mott, Proc. Phys. Soc. London Sect. A **62**, 415 (1949).
[2] J. Zaanen, G. A. Sawatzky, and J. W. Allen, Phys. Rev. Lett. **55**, 418 (1985).
[3] Z.-X. Shen, C. K. Shih, O. Jepsen, W. E. Spicer, I. Lindau, and J. W. Allen, Phys. Rev. Lett. **64**, 2442 (1990).
[4] Z.-X. Shen, R. S. List, D. S. Dessau, B. O. Wells, O. Jepsen, A. J. Arko, R. Barttlet, C. K. Shih, F. Parmigiani, J. C. Huang, and P. A. P. Lindberg, Phys. Rev. B **44**, 3604 (1991).
[5] W. Metzner and D. Vollhardt, Phys. Rev. Lett. **62**, 324 (1989); G. Kotliar and D. Vollhardt, Phys. Today **57**, No. 3, 53 (2004); G. Kotliar, S. Y. Savrasov, K. Haule, V. S. Oudovenko, O. Parcollet, and C. A. Marianetti, Rev. Mod. Phys. **78**, 865 (2006).
[6] K. Held, I. A. Nekrasov, G. Keller, V. Eyert, N. Blümer, A. K. McMahan, R. T. Scalettar, T. Pruschke, V. I. Anisimov, and D. Vollhardt, Phys. Status Solidi B **243**, 2599 (2006); K. Held, I. A. Nekrasov, G. Keller, V. Eyert, N. Blümer, A. K. McMahan, R. T. Scalettar, T. Pruschke, V. I. Anisimov, and D. Vollhardt, Psi-k Newsletter **56**, 65 (2003).
[7] F. C. Zhang and T. M. Rice, Phys. Rev. B **37**, 3759 (1988).
[8] A. Fujimori, F. Minami, and S. Sugano, Phys. Rev. B **29**, 5225 (1984).
[9] H. Eskes, M. B. J. Meinders, and G. A. Sawatzky, Phys. Rev. Lett. **67**, 1035 (1991).
[10] L. F. Mattheiss, Phys. Rev. B **5**, 290 (1972).
[11] K. Terakura, T. Oguchi, A. R. Williams, and J. Kübler, Phys. Rev. B **30**, 4734 (1984).
[12] V. I. Anisimov, J. Zaanen, and O. K. Andersen, Phys. Rev. B **44**, 943 (1991).
[13] A. Svane and O. Gunnarsson, Phys. Rev. Lett. **65**, 1148 (1990).
[14] S. Y. Savrasov and G. Kotliar, Phys. Rev. Lett. **90**, 056401 (2003).
[15] F. Manghi, C. Calandra, and S. Ossicini, Phys. Rev. Lett. **73**, 3129 (1994); J. Lægsgaard and A. Svane, Phys. Rev. B **55**, 4138 (1997).
[16] F. Aryasetiawan and O. Gunnarsson, Phys. Rev. Lett. **74**, 3221 (1995).
[17] S. V. Faleev, M. van Schilfgaarde, and T. Kotani, Phys. Rev. Lett. **93**, 126406 (2004); J.-L. Li, G.-M. Rignanese, and S. G. Louie, Phys. Rev. B **71**, 193102 (2005).
[18] J. E. Hirsch and R. M. Fye, Phys. Rev. Lett. **56**, 2521 (1986).
[19] J. Kuneš, V. I. Anisimov, A. V. Lukoyanov, and D. Vollhardt, Phys. Rev. B **75**, 165115 (2007).
[20] X. Ren, I. Leonov, G. Keller, M. Kollar, I. Nekrasov, and D. Vollhardt, Phys. Rev. B **74**, 195114 (2006).
[21] O. Tjernberg, S. Söderholm, G. Chiaia, R. Girard, U. O. Karlsson, H. Nylén, and I. Lindau, Phys. Rev. B **54**, 10 245 (1996).
[22] M. Jarrell and J. E. Gubernatis, Phys. Rep. **269**, 133 (1996).
[23] J. Eroles, C. D. Batista, and A. A. Aligia, Phys. Rev. B **59**, 14 092 (1999).
[24] J. Bała, A. M. Oleś, and J. Zaanen, Phys. Rev. Lett. **72**, 2600 (1994).
[25] J. Bała, A. M. Oleś, and J. Zaanen, Phys. Rev. B **61**, 13 573 (2000).